

Oxidation of Aromatic Aldehydes to Esters: A Sulfate Radical Redox System

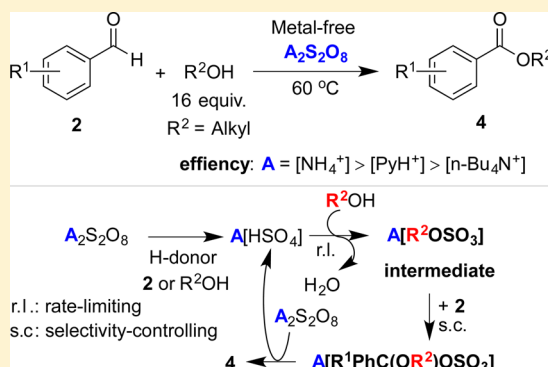
Ya-Fei Guo,^{†,‡} Sajid Mahmood,^{†,‡} Bao-Hua Xu,^{*,†} Xiao-Qian Yao,^{||,†} Hong-Yan He,^{||,†} and Suo-Jiang Zhang^{*,†}

[†]Beijing Key Laboratory of Ionic Liquids Clean Process, Key Laboratory of Green Process and Engineering, State Key Laboratory of Multiphase Complex Systems, Institute of Process Engineering, Chinese Academy of Sciences, Beijing 100190, PR China

[‡]College of Chemistry and Chemical Engineering, University of Chinese Academy of Sciences, Beijing 100049, PR China

Supporting Information

ABSTRACT: A mild oxidative esterification of various aromatic aldehydes by sulfate radical redox system was presented. In the reaction pathway exploration, the transiency of MeOSO_3^- was disclosed, which was generated from esterification between the in situ generated HSO_4^- and MeOH, a rate-limiting step in the process. More importantly, the selectivity-controlling step was represented by the subsequent nucleophilic displacement between MeOSO_3^- and aldehydes. The ionic oxidant **1a** ($(\text{NH}_4)_2\text{S}_2\text{O}_8$) with more N–H numbers in the cation, as compared with **1c** ($(n\text{-Bu}_4\text{N})_2\text{S}_2\text{O}_8$) and **1d** ($(\text{PyH})_2\text{S}_2\text{O}_8$), has better performance in the oxidative esterification of aldehydes.



INTRODUCTION

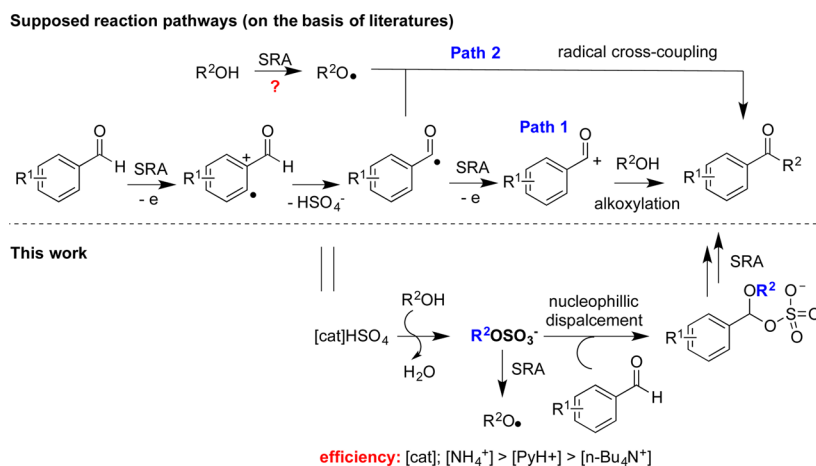
The significance and omnipresence of carboxylic esters in organic chemistry, pharmaceutical chemistry, and materials science has forced scientists to develop efficient methods for their preparation.¹ Esters are generally prepared via activation of acids or their carboxylic derivatives followed by nucleophilic substitution.² Instead of such two-steps operation containing oxidation and C–O bond formation, direct oxidative esterification of aldehydes with alcohols is a conceptually and economically attractive approach and has received increasing attention.³ Both carbonyl activation^{4–8} and direct formyl C–H activation strategies⁹ have been extensively investigated. However, challenges still remain, especially in the case of radical oxidative cross-coupling. One of the key issues is the relatively weak C–H bond in the formyl group of aldehydes is sensitive to electron transfer reagents and the undesired decarboxylation often happens beyond the dehydrogenative C–O cross coupling.¹⁰ Moreover, making the situation worse, alkanols are easily transformed to the corresponding aldehydes (further to acids) or ketones through radical mechanisms.¹¹ Up to now, the expected C–O cross-coupling of aldehydes with alkanols could be classified into two general types: (a) nucleophilic addition of alkoxy moiety (–OR) to aldehydes directly from alkanols mediated by various acids;^{5b,f} (b) through a chelating ligand of the M–OR (M = Pd, Ni et al.) complexes.^{5a,c,9a} In comparison, the other two potential models, radical cross coupling and alkoxylation of acyl cation with liberation of proton, were scarcely reported.¹²

Sulfate radical redox systems are involved in many oxidation and electron transfer processes,^{13,14} which herein are used to study the dehydrogenative coupling of aromatic aldehydes and alcohols. The reactivity of SRA (sulfate radical anion, $\text{SO}_4^{\cdot-}$) toward aromatics¹⁵ and alkanols¹⁶ may render the desired oxidative esterification of aromatic aldehydes unexpected pathways. For instance, one electron oxidation of the aromatics by SRA was reported to generate aromatic radical cations (even in the case of electron poor aromatic compounds, such as benzoic acid and aromatic ketones).¹⁵ In the case of aromatics substituted by formyl group under study, it is prone to liberate one proton in the subsequent step when no other reaction paths are available, with generating the corresponding acyl radicals.^{10a,17} Thus formed acyl radicals were expected to undergo a second one-electron oxidation by SRA with conversion to acyl cations in the light of Lin and Sen's study on radical carboxylation of methane,¹⁸ therefore, making the model of alcoholysis of acyl cation probable (path 1, Scheme 1). Independently, the radical cross-coupling (path 2, Scheme 1) may also be possible since the oxygen centered radicals were once detected in the spin-trap experiments of reactions of peroxydisulfates with alkanols.¹⁹ The unresolved question for path 2 is the O–H group in alkanols is a poor hydrogen atom donor and H-abstraction generally occurs on the alkyl moiety rather than the O–H group (BDE: CH_3OH , 96.06 ± 0.15 kcal/mol; CH_3OH , 104.6 ± 0.7 kcal/mol).^{16,20} The interpretation of

Received: November 20, 2016

Published: January 23, 2017

Scheme 1. Supposed Reaction Pathway and the One Disclosed by This Work



formation and fate of alkoxy radicals in the oxidation process warrant further study.

To better understand the reactivity of SRA, we have synthesized and characterized several organic salts of S₂O₈²⁻ with different cationic structure. Interestingly, their performances in the oxidative esterification of aromatic aldehydes vary significantly. The reaction pathway was explored and, to our surprise, neither of the supposed was tenable (two supposed pathways in Scheme 1). Both of the kinetic selectivity-controlling and rate-determining steps were freshly pointed out.

RESULTS AND DISCUSSION

Our study initiated with oxidative esterification of benzaldehyde (PhCHO, **2a**) in the presence of two commercially available oxidants, respectively, (NH₄)₂S₂O₈ (**1a**) and K₂S₂O₈ (**1b**). **1a** performed much better with a high aldehyde conversion and ester selectivity, which resulted in a 97% yield of **4aa** (Table S1). In sharp contrast, only traces of **4aa** were obtained in the case of **1b** as the oxidant. It might be attributed to the differences in the solubility of oxidants as reported²¹ (the aqueous solubility at 20 °C: **1a** 522 g/L²² vs **1b** 47 g/L²³). Based on this point, (*n*-Bu₄N)₂S₂O₈ (**1c**), which was supposed to perform better than or at least comparable as **1a** with an increased solubility in MeOH by incorporating four butyl chains into the cation unit, was prepared.²⁴ However, the reaction in the case of **1c** as the oxidant preferably generated carboxylic acid **5aa** in a selectivity of 32%, nearly four times higher than that of desired ester formed. The next efforts on synthesis of ammonium oxidants (^{*m*}Bu_{*m*}H_{4-*m*}N)₂S₂O₈ (*m* = 1, 2 or 3) were proven failures, while their pyridinium analogue (PyH)₂S₂O₈ (**1d**) was finally obtained through ion exchange between pyridine hydrochloride (PyHCl) and **1b**. Compound **1d** features a typical pyridinium NMR resonance in DMSO-*d*₆ [δ ¹H (Py): 8.93 (2H), 8.60 (1H), and 8.07 (2H) ppm, δ ¹³C{¹H}: 147.0, 142.1, 127.7 ppm]. The X-ray single crystal diffraction displays a layered ionic arrangement with one central S₂O₈²⁻ dianion and two separated protonated pyridine (PyH⁺) as the counterion (Figure S2). The reaction by using **1d** as an oxidant resulted in a moderate ester selectivity of 78% compared with those obtained by the other oxidants screened (**1a**: 97% and **1c**: 9%).

Various aromatic aldehydes were then reacted, by using 1.5 mol equiv of **1a** as the oxidant, with 16 equiv of alkanols at 60 °C (Table 1). It offered excellent yield of the expected ester in

Table 1. Oxidative Esterification of Aromatic Aldehydes with Alcohols by **1a**^a

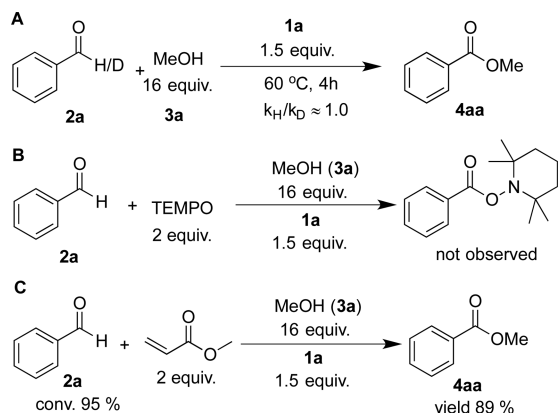
entry	substrate 2 (R ¹)	substrate 3 (R ²)	time (h)	4 (yield (%)) ^b
1	2a (H)	3a (Me)	4.0	4aa (97%)
2	2b (<i>p</i> -NO ₂)	3a (Me)	2.5	4ba (99%)
3	2c (<i>p</i> -OMe)	3a (Me)	16.0	4ca (14%) ^c
4	2d (<i>p</i> -Me)	3a (Me)	2.5	4da (97%)
5	2e (<i>m</i> -Cl)	3a (Me)	2.5	4ea (94%)
6	2f (<i>m</i> -Me)	3a (Me)	3.0	4fa (87%)
7	2a (H)	3b (<i>n</i> -Et)	24.0	4ab (98%)
8	2a (H)	3c (<i>n</i> -Bu)	48.0	4ac (99%)
9	2a (H)	3d (<i>i</i> -Pr)	24.0	4ad (85%)
10	2a (H)	3e (<i>t</i> -Bu)	16.0	4ae (21%)
11	2a (H)	3f (PhCH ₂)	8.0	4af (82%)
12	2a (H)	3g (Ph)	8.0	4ag (8%) ^d

^aGeneral conditions: **2** (1 mmol), **3** (16 mmol), **1a** (1.5 mmol), 60 °C. ^bIsolated yields. ^c4-Methoxyphenol was mainly obtained in a yield of 80%. ^dYields determined by GC-MS through using areas of peak normalization method.

most cases (entry 1–2, 4–9). Peculiarly, those bearing electron-rich groups such as *p*-anisaldehyde provided 4-methoxyphenol as the major product in 80% yields (entry 3). Besides, the bulky alcohol also performed poorly (entry 10). Noteworthy, the reaction with phenol (**3g**) was nearly suppressed (entry 12) probably because it is a radical scavenger.

As posited in Scheme 1, both the alkoxylation of acyl cation (path 1) and radical cross coupling (path 2) experience the same transiency of acyl radical. In experiments, the obtained kinetic isotope value ($k_H/k_D \approx 1.0$) from the independent esterification of benzoic aldehyde versus benzoic aldehyde-*d*₁ indicates the cleavage of formyl C–H bond is not the turnover-limiting step (Scheme 2A). However, efforts on trapping benzyl acyl or its derived benzyl radical by 2,2,6,6-tetramethylpiperidinoxy (TEMPO) from the reaction of **2a** and **3a**²⁵ under standard reaction conditions were proven unsuccessful (Scheme 2B). The formation of ester proceeded quantitatively with the use of methyl acrylate as the potential trapper of acyl radical (Scheme 2C), thus disfavoring an acyl radical pathway.

Scheme 2. Mechanistic Studies



To elucidate the oxidative esterification pathway, the spin-trapping technique was introduced to detect the involved but short-lived radicals, wherein the dimethylpyridine *N*-oxide (DMPO) was used as the spin-trap reagent. By in situ electron spin resonance (ESR) study of a MeOH solution of **1a** and **2a** (under air, see SI for the detail), it features a typical DMPO-OMe resonance²⁶ at $a^N = 13.3$ G, $a^{H\beta} = 9.4$ G (Figure 1A)

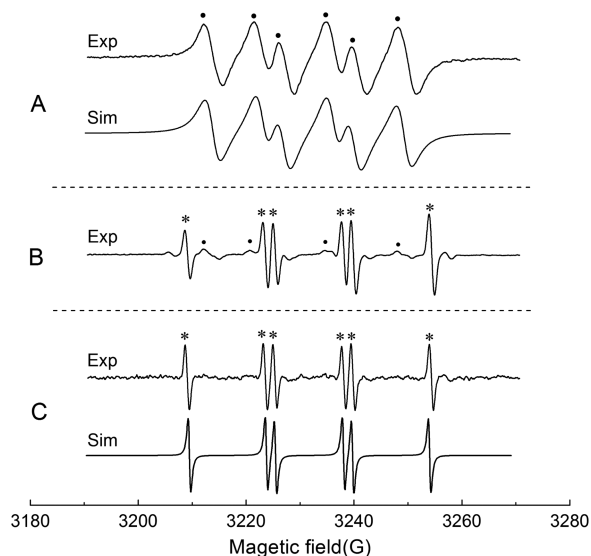


Figure 1. ESR spectra of spin-trap experiment of **1a** and **2a** in MeOH. (A) 4 min, with the simulation spectra (bottom, $a^N = 13.3$ G, $a^{H\beta} = 9.4$ G); (B) 12 min; (C) 16 min, with the simulation spectra (bottom, $a^N = 14.5$ G, $a^{H\beta} = 16.2$ G).

other than the carbon centered adduct of DMPO (DMPO-CH₂OH) after reaction at 60 °C for 4 min. Subsequently, another signal at $a^N = 14.5$ G, $a^{H\beta} = 16.2$ G quickly emerged and gradually surpassed (Figure 1B, C). The spectral parameters quoted for the second, obtained by the simulation of ESR spectra (Figure 1C), were assigned to an unreported DMPO-hemiacetal. Compared with the hyperfine coupling constants of DMPO-OMe, it has a larger $a^{H\beta}$ parameter at 16.2 G, which might be attributed to a perpendicular β -H to NO \cdot unit of DMPO caused by steric forces of the *i*-OMe substituent.

The structure assumption for the radical adducts detected by in situ ESR was further confirmed by ultraperformance liquid chromatography coupled with electrospray ionization tandem

mass spectrometry (UPLC-ESI-MS) technique. Besides the DMPO-OMe eluted at 0.7 min in an oxidized form with a mass signal at m/z 144.10 (calcd HRMS (ESI) exact mass for $[M+H]^+$ (C₇H₁₄NO₂): m/z 144.10, Figure 2B), the peak assigned to the DMPO-hemiacetal was also observed. ESI analysis of the elution at 12.6 min indicates it is again an oxidized form with molecular weight at m/z 250.14 (calcd HRMS (ESI) exact mass for $[M+H]^+$ (C₁₄H₂₀NO₃): m/z 250.14, Figure 2C), while the fragment peak at m/z 129.09 was attributed to the breaking C–O bond of hemiacetal unit and generation of the oxidized DMPO moiety (calcd HRMS (ESI) exact mass for (C₆H₁₁NO₂): m/z 129.08, Figure 2C).

To declare if the hydrogen abstraction had ever occurred on the methyl group as expected, a 1:1 mixture of CD₃OH and **2a** was then treated with **1a**. However, neither D/H exchange nor kinetic isotope effect (KIE; $k_H/k_D = 0.94$ (≈ 1.0)) was obtained (Figure S8). Independent to this, the negative mode ESI analysis of the reaction solution of **1a/1d** and MeOH under the standard condition shows peaks at m/z 96.96 (assigned to HSO₄[−]) and 110.98 (assigned to MeOSO₃[−], a monomethyl sulfate analogue from reaction of HSO₄[−] and MeOH). These newly formed methyl sulfate salts (**6a** and **6d**) were finally isolated and the solid state of the anion moiety was confirmed by X-ray single crystal diffraction study in the pyridinium case (**6d**, Figure 3). Importantly, a mass signal of DMPO-OMe in an oxidized form at m/z 144.10 was detected in the reaction of **6d** with **1a** at 60 °C in THF, suggesting the methyl sulfate species are precursors of MeO \cdot trapped in ESR experiments.

The subsequently trapped hemiacetal radical was then formally attributed to the nucleophilic addition of MeO \cdot at the formyl carbon of PhCHO (Scheme 3B). However, by DFT calculations with the consideration of solvent effect (Figure S9), the hydrogen abstraction of PhCHO by MeO \cdot was investigated to proceed easily with a comparatively lower energy barrier (calcd 3.47 kcal/mol, Scheme 3A). Although the ester formation by radical cross-coupling was proven to be spontaneous, neither the benzyl acyl radical nor its decarboxylated derivative was trapped by radical inhibitors (DMPO/TEMPO/methyl acrylate) in our experiments. In fact, monitored by in situ NMR, the reaction of **6a** with **2a** in the absence of oxidants proceeded immediately in methanol even at room temperature, while directly and qualitatively generating the corresponding acetal (PhCH(OMe)₂, Figure S11). It was reasonably attributed to two sequential steps of electrophilic alkylation as depicted in Scheme 3. The intermediate **7** was formed by nucleophilic displacement between methyl sulfate salt **6** and aldehyde (Scheme 3C), which was prone to release the corresponding hemiacetal radical (detected by spin-trap experiments) upon reaction with SRA. However, at this point, the alternative pathway leading to **7** from stepwise nucleophilic substitution could not be completely ruled out (Scheme 3D).

A key insight into ester formation is revealed by monitoring the selectivity for C–H esterification of a series of *para*-substituted benzaldehydes via competition experiments, in which an equimolar quantity of a *para*-substituted benzaldehyde and unsubstituted benzaldehyde, were added in the **1a**/MeOH system. The resulted products distribution was measured by gas chromatography (GC) at early reaction times. Electron-donating groups greatly enhance the selectivity for C–H esterification, with generating a negative Hammett slope ($\rho = -1.5$, $R^2 = 0.99$, Figure 4). This moderate value is in line with a free-radical mechanism rather than considerable positive charge development on the aromatic hydrocarbons in

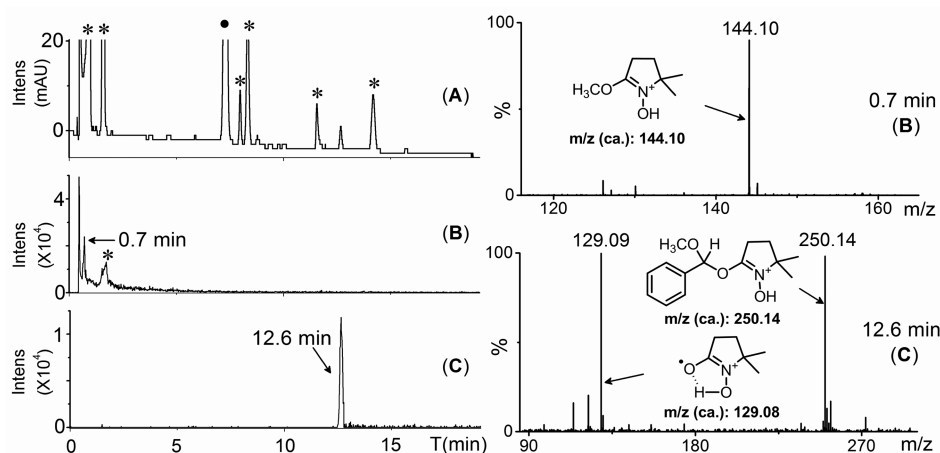


Figure 2. UPLC-ESI-MS analysis of spin-trap experiment of **1a** and **2a** in MeOH. (A) UV trace, (B) reconstituted ion chromatograms for m/z 144.10, and (C) 250.14. Other signals in A can be attributed to UV-chromatography of the substrates, DMPO (*) and to **2a** (•).

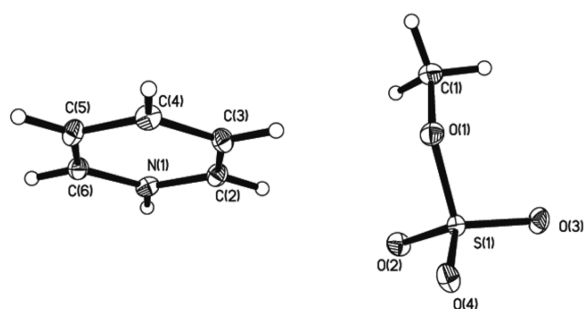
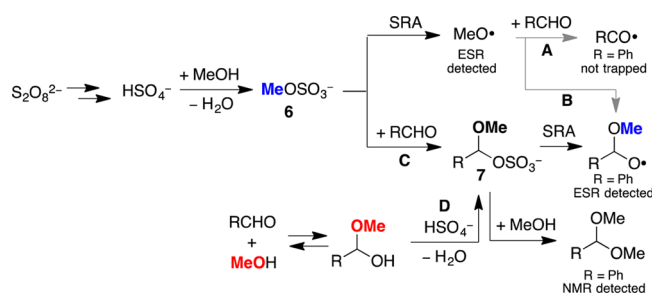


Figure 3. ORTEP of the intermediate **6d** (PyHMeOSO₃) represented at the 30% probability level from the X-ray single crystal structure. Hydrogen atoms are included but unlabeled for clarity.

Scheme 3. Proposed Key Steps for the Oxidative Esterification of Aldehydes



the transition state. It can be rationalized by preferential formation of **7** derived from the electron-rich aldehydes since the cleavage of C–H bond is not the turnover-limiting step (indicated by the kinetic isotope experiment). Therefore, electrophilic alkylation between **6** and aldehydes sounds more probable for the route to **7**, thereby kinetically controlling the selectivity.

Before the reaction pathway well settled, it is necessary to understand the origin for the peculiar Dakin-type product from *p*-OMe-PhCHO (**2c**) in Table 1. As it demonstrated, even under argon, 4-methoxyphenol was mainly formed (Scheme 4A). Nucleophilic substitution of the potentially generated aromatic radical cations (formed via one electron oxidation of the aromatics by SRA) was immediately excluded since no 1,4-dimethoxybenzene was detected in the presence of abundant

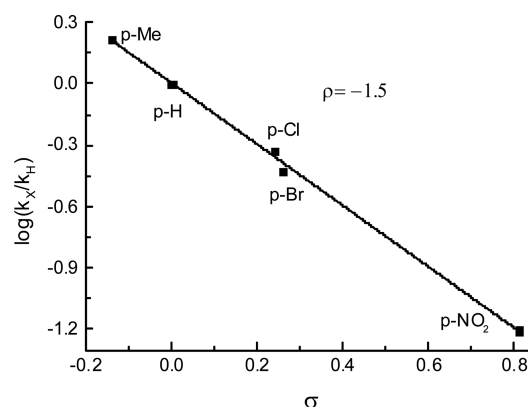
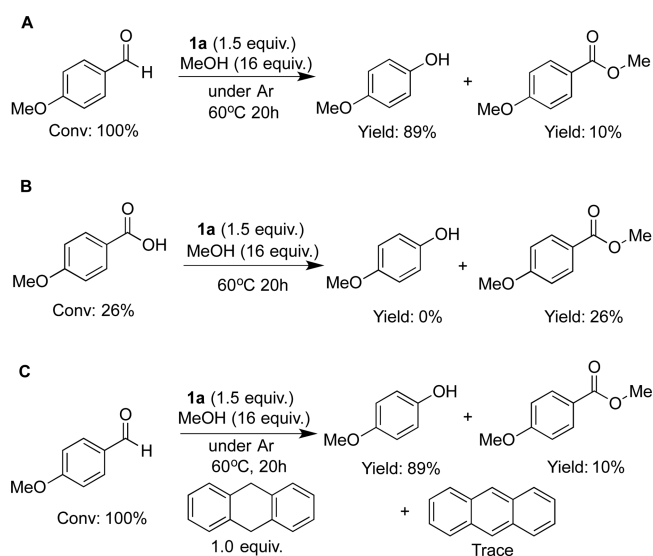


Figure 4. Relative reactivities of *para*-substituted benzaldehydes in **1a**/MeOH system.

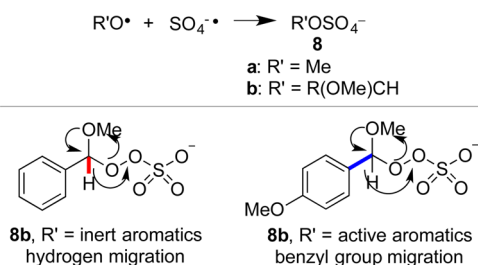
Scheme 4. Control Experiments



MeOH as nucleophiles (more stronger than H₂O). The well-known pathway derived from H₂SO₅ (Caro's acid) is unlikely since the system under study is a neutral to weak acidic oxidation process,^{27–29} not up to the requirements for generation of H₂SO₅ from S₂O₈²⁻.

We then conducted the reaction in the presence of 9,10-dihydroanthracene, a potential trap for alkoxy radical (BDE: $C(sp^3)-H_{(9,10\text{-dihydroanthracene})}$: 76.3 kcal/mol; $MeO-H$: 104.6 ± 0.7 kcal/mol),²⁰ which forms only traces of anthracene (Scheme 4C), while the reaction leading to 4-methoxyphenol was not affected at all. It demonstrates either methoxyl or hemiacetal radical, if formed, would be quickly trapped by SRA via radical cross-coupling, while leading to a new type of peroxosulfate product **8** (Scheme 5). A similar termination by

Scheme 5. Formation of Peroxosulfate **8 and Two Reaction Modes in the Case of **8b****



SRA was discovered for $HO\cdot$, which subsequently produced HSO_4^- and O_2 .²⁹ Following the Baeyer–Villiger reaction rules, either the corresponding ester or phenol could be produced from **8b** depending on the electrophilicity of the R group inside. For instance, substituted by electron donating substituent, the aromatic benzyl rather than the hydrogen would migrate, thereby generating phenol as the major product.

Cross experiments further indicated the generation of methyl sulfate salts **6** (Scheme 3) proceeded comparatively slower (Figure S11–14) and was therefore regarded as the rate-determining. To understand the reaction route further, especially the ways that different oxidant operate, we then turned our attention to the details leading to **6** under a neutral oxidation process. Previous studies demonstrated that the effect of organic substances on the rate of decomposition of $S_2O_8^{2-}$ is striking. For instance, Bartlett and Cotman disclosed the decomposition rate of $K_2S_2O_8$ was increased by 25-fold in the presence of MeOH, with quantitatively transforming methanol to formaldehyde.³⁰ In this study, the rate constant of decomposition of **1a** and **1d** (0.015 M) in the presence of MeOH (0.5 M) at 80 °C were evaluated, respectively. The kinetics more closely approximate the 2/3 order (Figure 5A)

than it does first order (note that the decomposition at 79.8 °C in aqueous solution at pH 8 is strictly of the first order).³⁰ Most importantly, the difference between the oxidants (ca. **1a**: 1.48; **1d**: 0.38 ($M^{-1/2}\cdot\text{min}^{-1}$)) was found remarkable in the presence of a solvent scale of H-bond donors, such as a mixture of methanol and water (both at a completely dissolved status).

The question pending in the route to reach **6** was if the esterification between MeOH and HSO_4^- is fast enough to be ignored. Where possible, rate constants were independently evaluated and determined. Dry MeOH was mixed with three different HSO_4^- salts in CD_3CN and heated to 60 °C. Equilibrium was not reached within 80 min in three cases, all resulting in a limited conversion of HSO_4^- to $MeOSO_3^-$ salts (<40%). The $MeOSO_3^-$ peak integral (CH_3 , NH_4^+ : 3.62 ppm; PyH^+ : 3.63 ppm; $n-Bu_4N^+$: 3.56 ppm) was normalized to the methyl peak resonance of the MeOH solvent and the initial second-order forward rate constants were calculated from the peak-integral data. Results demonstrated that these reactions proceeded with rate constants of the order of $10^{-4} M^{-1}\cdot\text{min}^{-1}$ and $n-Bu_4NHSO_4$ is relatively poor agent in the esterification (Figure 5B, k ($M^{-1}\cdot\text{min}^{-1}$), NH_4^+ : 1.64×10^{-3} ; PyH^+ : 8.41×10^{-4} ; $n-Bu_4N^+$: 1.98×10^{-4}). Nearly 10^4 times gap in the calculated rate constant between the decomposition of $S_2O_8^{2-}$ and subsequent esterification renders the later a rate-limiting step.

CONCLUSION

In this study, we presented mild oxidative esterification of various aromatic aldehydes by sulfate radical redox system. The reaction pathways, especially the kinetic selectivity-controlling and rate-determining steps, have been fully discussed. The supposed step of converting aromatic aldehydes to acyl radical via aromatic radical cation may occur at the initial stage, with generating HSO_4^- for the oxidation process. But, it was not absolutely essential to use aldehydes as the sacrifice. Neither of the expected alkoxylation of acyl cation or radical cross-coupling was tenable in the formation of ester. Instead, the transiency of $MeOSO_3^-$ was disclosed, which was generated from esterification between HSO_4^- and MeOH, a rate-limiting step in the oxidative cross-coupling process. It readily generates methoxyl radical upon reacting $MeOSO_3^-$ with SRA, thereby the contradiction between the theoretic analysis and spin-trap experiments on the origin of alkoxy radical from reaction of SRA and alkanols was well answered. Moreover, the important selectivity-controlling step was attributed to the subsequent

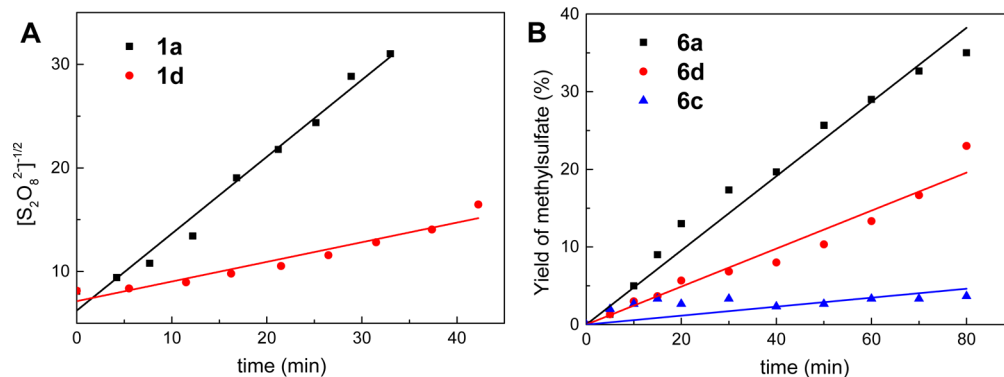


Figure 5. (A) Decomposition of the persulfate **1a** and **1d** (0.015 M) at 80 °C in the presence of 0.5 M methanol aqueous solution monitored by titration, plotted as a 3/2 order reaction (left), and the reaction rate constant were calculated as twice the slope. (B) The esterification between MeOH (0.29 M) and HSO_4^- (0.015 M) at 60 °C monitored by *in situ* NMR (right), and the initial reaction rate constant were calculated accordingly.

nucleophilic displacement between MeOSO_3^- and aldehyde in this study. Although the structure-effect relationship in terms of the oxidants was not formulated, the ionic oxidant **1a** with more N–H numbers in the cation, as compared with **1c** and **1d**, proceeded better in the oxidative esterification of aldehydes.

EXPERIMENTAL SECTION

General Procedures. All reactions were done under air and the solvents were not dried unless otherwise noted. The task specific oxidant $(\text{Bu}_4\text{N})_2\text{S}_2\text{O}_8$ (**1c**) was prepared according to the literature (Yang, S. G.; Hwang, J. P.; Park, M. Y.; Lee, K.; Kim, Y. H. *Tetrahedron* **2007**, *63*, pp 5184–5188). NMR spectra were recorded on a 600 MHz; spectrometer. ^1H NMR and ^{13}C NMR, chemical shift δ was given relative to TMS and referenced to the solvent signal. Column chromatography was performed using silica gel. Analytical TLC was done using precoated silica gel 60 F₂₅₄ plates. Melting points were determined from differential scanning calorimetry (DSC) data, which were obtained in sealed aluminum pans with a heating rate of 10 °C/min. Fourier transform infrared (FTIR) data were collected with anhydrous KBr as standard. Thermogravimetric (TG) analysis was operated at a heating rate of 5 °C/min under N_2 atmosphere using an empty crucible as the reference. The ultraperformance liquid chromatography system was equipped with TUV detector and a ACQUITY UPLC BEH C18 column (2.1 × 50 mm, 1.7 μm). ESI-MS analysis was performed on a time-of-flight mass spectrometer using an electrospray ionization (ESI) source.

The crystal structure analysis was performed on a CCD X-ray diffractometer equipped with an area detector, and the crystals were irradiated using graphite monochromated Mo K α radiation ($\lambda = 0.7103 \text{ \AA}$). Data collection was performed and the unit cell was initially refined using APEX2 (Bruker, APEX2 v2010.3–0 ed., Bruker AXS Inc., Madison, 2010). Data reduction was performed using SAINT (Bruker, SAINT v7.68A ed., Bruker AXS Inc., Madison, 2009) and XPREF (Bruker, XPREF v2008/2 ed., Bruker AXS Inc., Madison, 2008). Absorption corrections were applied using SADABS (Bruker1, SADABS v2008/1 ed., Bruker AXS Inc., Madison, 2008). The structure was solved and refined with the aid of the SHELXTL software package (Bruker4, SHELXTL v2008/4 ed., Bruker AXS Inc., Madison, 2008). The full-matrix least-squares refinement on F^2 included atomic coordinates and anisotropic thermal parameters for all non-hydrogen atoms. The hydrogen atoms were included using a riding model. CCDC 1013691 (**1a**, $(\text{NH}_4)_2\text{S}_2\text{O}_8$), 1014063 (**1d**, $(\text{PyH})_2\text{S}_2\text{O}_8$), and 1013692 (**6d**, MeOSO_3PyH) contain the supplementary crystallographic data for this paper. These data can be obtained free of charge at www.ccdc.cam.ac.uk/conts/retrieving.html.

Recrystallization of 1a ($(\text{NH}_4)_2\text{S}_2\text{O}_8$). A saturated aqueous solution of commercial **1a** at 50 °C was cooled down to room temperature, from which crystals of **1a** suitable for X-ray structure analysis were slowly obtained. mp 187 °C (dec). IR (KBr) [cm^{-1}] = 3159 (vs); $\nu = 2352$ (vw); 1402 (s); 1298 (s); 1264 (s); 1057 (s); 689 (s); 621 (m); 593 (w); 559 (s); 432 (vw).

Preparation of 1c ($(\text{Bu}_4\text{N})_2\text{S}_2\text{O}_8$). Tetra-butylammonium hydrogensulfate (Bu_4N)HSO₄ (14.1 g, 0.04 mol) and $\text{K}_2\text{S}_2\text{O}_8$ (5.43 g, 0.02 mol) were dissolved in 100 mL of distilled water and the solution was stirred for 30 min at room temperature. The mixture was then extracted with CH_2Cl_2 (20 mL × 3), and the combined organic layers were washed with distilled water (20 mL × 3), dried over anhydrous MgSO_4 , and filtered. Evaporation of the solvent in vacuo and subsequent drying under high vacuum gave a white solid of **1c** in 80% yield. mp 115 °C (dec); Anal. Calcd for $\text{C}_{32}\text{H}_{72}\text{N}_2\text{O}_8\text{S}_2$: C, 56.77; H, 10.72; N, 4.14; S, 9.47. Found: C, 56.42; H, 10.58; N, 4.16; S, 9.21. IR (KBr) [cm^{-1}] = 3424 (s); 2961 (s); 2940 (w); 2874 (w); 1624 (w); 1487 (w); 1467 (w); 1382 (vw); 1298 (s); 1278 (s); 1152 (vw); 1062 (m); 1041 (w); 884 (vw); 728 (w); 703 (m); 621 (w); 591 (vw); 562 (w); ^1H NMR (600 MHz, CDCl_3 , 298 K): $\delta = 3.30$ (m, 2H, N– CH_2), 1.63 (m, 2H, CH_2), 1.44 (m, 2H, CH_2), 0.97 (t, $^3J_{\text{HH}} = 7.4$ Hz, 3H, CH_3). $^{13}\text{C}\{^1\text{H}\}$ NMR (151 MHz, CDCl_3 , 298 K) $\delta = 58.6$ (N– CH_2), 24.1 (CH_2), 19.8 (CH_2), 13.8 (CH_3).

Preparation of 1d. An acetonitrile (100 mL) suspension of PyHCl (4.72 g, 0.04 mol) and $\text{K}_2\text{S}_2\text{O}_8$ (5.43 g, 0.02 mol) was stirred at room temperature for 24 h and then filtered. The solvent of filtrate was removed under rotate machine and the residue was recrystallized from methanol at –15 °C to give white crystals (5.29 g, 75%). Crystals suitable for single X-ray diffraction were obtained from recrystallization in methanol at –15 °C. mp 57.5 °C. Anal. Calcd for $\text{C}_{10}\text{H}_{12}\text{N}_2\text{O}_8\text{S}_2$: C, 34.09; H, 3.43; N, 7.95; S, 18.20. Found: C, 34.13; H, 3.36; N, 7.99; S, 17.80. IR (KBr) [cm^{-1}] = 3423 (s); 3134 (vw); 3064 (w); 2956 (vw); 2801 (vw); 1636 (w); 1611 (w); 1537 (vw); 1486 (m); 1299 (vs); 1271 (s); 1199 (vw); 1117 (w); 1062 (s); 728 (w); 703 (m); 681 (m); 619 (vw); 592 (w); 562 (m). ^1H NMR (600 MHz, $\text{DMSO}-d_6$, 298 K): $\delta = 8.93$ (dd, $^3J_{\text{HH}} = 6.4$ Hz, $^4J_{\text{HH}} = 1.3$ Hz, 2H, Py), 8.60 (tt, $^3J_{\text{HH}} = 7.8$ Hz, $^4J_{\text{HH}} = 1.3$, 1H, *p*-Py), 8.07 (tm, $^3J_{\text{HH}} = 7.8$ Hz, 2H, Py), N.O. (br s, 1H, N–H). $^{13}\text{C}\{^1\text{H}\}$ NMR (151 MHz, $\text{DMSO}-d_6$, 298 K): 147.0, 142.1, 127.7 (Py).

Preparation of 6a ($\text{NH}_4\text{MeOSO}_3$). A methanol (50 mL) suspension of $(\text{NH}_4)_2\text{S}_2\text{O}_8$ (4.56 g, 0.02 mol) was stirred and refluxed under argon for 24 h and then filtered. The filtrate was crystallized at –15 °C and the crystals obtained were recrystallized from methanol for two times to give white crystals (0.45 g, 8%). The HSO[–] signal was no longer present in the ESI-MS spectrum with negative mode. Anal. Calcd for $\text{CH}_7\text{NO}_4\text{S}$: C, 9.30; H, 5.46; N, 10.85; O, 49.56; S, 24.83. Found: C, 9.32; H, 5.45; N, 10.88; O, 49.58; S, 24.85. ^1H NMR (600 MHz, $\text{DMSO}-d_6$, 298 K): 7.09 (t, $^3J_{\text{HH}} = 51$ Hz, 4H, NH_4), 3.40 (s, 3H, CH_3). $^{13}\text{C}\{^1\text{H}\}$ NMR (151 MHz, $\text{DMSO}-d_6$, 298 K) 53.1 (CH_3).

Preparation of 6d (PyHMeOSO_3). A methanol (100 mL) suspension of PyHCl (4.62 g, 0.04 mol) and $\text{K}_2\text{S}_2\text{O}_8$ (5.41 g, 0.02 mol) was stirred and refluxed under argon for 24 h and then filtered. The filtrate was crystallized at –15 °C and the crystals obtained were recrystallized from methanol to give white crystals (1.58 g, 23%). Crystals suitable for single X-ray diffraction were obtained from recrystallization in methanol at –15 °C. Anal. Calcd for $\text{C}_9\text{H}_9\text{NO}_4\text{S}$: C, 37.69; H, 4.74; N, 7.33; O, 33.47; S, 16.77. Found: C, 37.71; H, 4.77; N, 7.30; O, 33.43; S, 16.79. ^1H NMR (600 MHz, $\text{DMSO}-d_6$, 298 K): $\delta = 8.95$ (dd, $^3J_{\text{HH}} = 6.6$ Hz, $^4J_{\text{HH}} = 1.6$ Hz, 2H, Py), 8.65 (tt, $^3J_{\text{HH}} = 7.8$ Hz, $^4J_{\text{HH}} = 1.5$, 1H, *p*-Py), 8.11 (tm, $^3J_{\text{HH}} = 7.21$ Hz, 2H, Py), N.O. (br s, 1H, N–H), 3.41 (s, 3H, CH_3). $^{13}\text{C}\{^1\text{H}\}$ NMR (151 MHz, $\text{DMSO}-d_6$, 298 K): 146.7, 142.2, 127.4 (Py), 53.1 (CH_3).

Decomposition of the Oxidants in the Presence of Methanol. Peroxodisulfate (**1a**, **1d**) was titrated by indirect iodometry. The sample to be analyzed was made 1 M in potassium iodide and one gram of sodium bicarbonate was dissolved in it. To this sample was added 20–25 mL of 10% sulfuric acid. During and after the liberation of the carbon dioxide, which provided a convenient means of sweeping out the oxygen, the solution stood in a glass-stoppered flask. After standing for 30 min in the dark at room temperature, the liberated iodine was titrated with standard thiosulfate. The reaction was carried out using a 150 mL stainless steel vessel with a sampling pipe. Solution of peroxodisulfate (150 mL, 0.015 M) in the presence of 0.5 M methanol was prepared. The first sample was took before heating and closing the vessel. And samples (7 mL) were taken every 4 min after heating. The rate constant was calculated according to the following eqs 1 and 2:

$$-\frac{dc}{dt} = kc^{2/3} \quad (1)$$

$$c^{-1/2} = \frac{k}{2}t + c_0^{-1/2} \quad (2)$$

Then the rate constant correspond to twice the slope of $c^{-1/2} \sim t$ plot.

Preparation of 4aa. A methanol suspension (0.65 mL, 16 mmol, 16 equiv) of benzaldehyde (0.11 g, 1 mmol, 1 equiv) and $(\text{NH}_4)_2\text{S}_2\text{O}_8$ (0.35 g, 1.5 mmol, 1.5 equiv) was stirred at 60 °C for 4 h. After cooling to room temperature, distilled water (10 mL) was used to dissolve the solid and the product was extracted by ethyl acetate (3 × 10 mL). The combined organic extract was concentrated and then purified by column chromatography on silica gel (petroleum ether/ethyl acetate 40:1) provided **4aa** in a yield of 96%. ^1H NMR (600 MHz, CDCl_3 ,

298 K): δ = 8.04 (dd, $^3J_{\text{HH}} = 8.3$ Hz, $^3J_{\text{HH}} = 1.3$ Hz, 2H, Ph), 7.54 (tt, $^3J_{\text{HH}} = 7.6$ Hz, $^3J_{\text{HH}} = 1.3$ Hz, 1H, *p*-Ph), 7.43 (ddm, $^3J_{\text{HH}} = 8.3$ Hz, $^3J_{\text{HH}} = 7.6$ Hz, 2H, Ph), 3.91 (s, 3H, OCH₃). $^{13}\text{C}\{^1\text{H}\}$ NMR (151 MHz, CDCl₃, 298 K): δ = 167.2 (C=O), 133.0, 130.3, 129.7, 128.4 (Ph), 52.2 (OCH₃).

Preparation of 4ba. A methanol suspension (0.65 mL, 16 mmol, 16 equiv) of 4-nitrobenzaldehyde (0.15 g, 1 mmol, 1 equiv) and (NH₄)₂S₂O₈ (0.35 g, 1.5 mmol, 1.5 equiv) was stirred at 60 °C for 2.5 h. After cooling to room temperature, distilled water (10 mL) was used to dissolve the solid and the product was extracted by ethyl acetate (3 × 10 mL). The combined organic extract was concentrated and then purified by column chromatography on silica gel (petroleum ether/ethyl acetate 20:1) provided **4ba** in a yield of 99%. ^1H NMR (600 MHz, CDCl₃, 298 K): δ = 8.27 (d, $^3J_{\text{HH}} = 8.3$ Hz, 2H, Ph), 8.19 (d, $^3J_{\text{HH}} = 8.3$ Hz, 2H, Ph), 3.97 (s, 3H, OCH₃). $^{13}\text{C}\{^1\text{H}\}$ NMR (151 MHz, CDCl₃, 298 K): δ = 165.3 (C=O), 150.6 (*i*-Ph), 135.60 (*i*-Ph), 130.8, 123.7 (Ph), 52.9 (OCH₃).

Preparation of 4ca. A methanol suspension (0.65 mL, 16 mmol, 16 equiv) of 4-methoxybenzaldehyde (0.14 g, 1 mmol, 1 equiv) and (NH₄)₂S₂O₈ (0.35 g, 1.5 mmol, 1.5 equiv) was stirred at 60 °C for 16 h. GC-MS analysis of the resulting solution indicated **4ca** and 4-methoxyphenol in a ratio of 1.0:6.0 was formed. After cooling to room temperature, distilled water (10 mL) was used to dissolve the solid and the product was extracted by ethyl acetate (3 × 10 mL). The combined organic extract was concentrated and then purified by column chromatography on silica gel (petroleum ether/ethyl acetate 2:1) provided **4ca** in a yield of 14% and the major product 4-methoxyphenol in a yield of 80%. For **4ca**: ^1H NMR (600 MHz, CDCl₃, 298 K): δ = 8.00 (dm, $^3J_{\text{HH}} = 8.9$ Hz, 2H, Ph), 6.92 (dm, $^3J_{\text{HH}} = 8.9$ Hz, 2H, Ph), 3.89, 3.86 (each s, each 3H, OCH₃). $^{13}\text{C}\{^1\text{H}\}$ NMR (151 MHz, CDCl₃, 298 K): δ = 167.0 (C=O), 163.5, 122.8 (each *i*-Ph), 131.7, 113.8 (each Ph), 55.6, 52.0 (each OCH₃). For 4-methoxyphenol: ^1H NMR (600 MHz, CDCl₃, 298 K): δ = 6.80 (dm, $^3J_{\text{HH}} = 9.3$ Hz, 2H, Ph), 6.77 (dm, $^3J_{\text{HH}} = 9.3$ Hz, 2H, Ph), 4.38 (br, 1H, OH), 3.77 (s, 3H, OCH₃). $^{13}\text{C}\{^1\text{H}\}$ NMR (151 MHz, CDCl₃) δ = 153.9, 149.6 (each *i*-Ph), 116.2, 115.0 (Ph), 56.0 (OCH₃).

Preparation of 4da. A methanol suspension (0.65 mL, 16 mmol, 16 equiv) of 4-methylbenzaldehyde (0.12 g, 1 mmol, 1 equiv) and (NH₄)₂S₂O₈ (0.35 g, 1.5 mmol, 1.5 equiv) was stirred at 60 °C for 2.5 h. After cooling to room temperature, distilled water (10 mL) was used to dissolve the solid and the product was extracted by ethyl acetate (3 × 10 mL). The combined organic extract was concentrated and then purified by column chromatography on silica gel (petroleum ether/ethyl acetate 20:1) provided **4da** in a yield of 97%. ^1H NMR (600 MHz, CDCl₃, 298 K): δ = 7.93 (dm, $^3J_{\text{HH}} = 8.2$ Hz, 2H, Ph), 7.22 (dm, $^3J_{\text{HH}} = 8.2$ Hz, 2H, Ph), 3.89 (s, 3H, OCH₃), 2.39 (s, 3H, CH₃). $^{13}\text{C}\{^1\text{H}\}$ NMR (151 MHz, CDCl₃, 298 K): δ = 167.2 (C=O), 143.6 (*i*-Ph), 129.7, 129.1 (Ph), 127.51 (*i*-Ph), 52.0 (OCH₃), 21.7 (CH₃).

Preparation of 4ea. A methanol suspension (0.65 mL, 16 mmol, 16 equiv) of 4-chlorobenzaldehyde (0.14 g, 1 mmol, 1 equiv) and (NH₄)₂S₂O₈ (0.35 g, 1.5 mmol, 1.5 equiv) was stirred at 60 °C for 2.5 h. After cooling to room temperature, distilled water (10 mL) was used to dissolve the solid and the product was extracted by ethyl acetate (3 × 10 mL). The combined organic extract was concentrated and then purified by column chromatography on silica gel (petroleum ether/ethyl acetate 20:1) provided **4ea** in a yield of 94%. ^1H NMR (600 MHz, CDCl₃, 298 K): δ = 7.95 (dm, $^3J_{\text{HH}} = 8.5$ Hz, 2H, Ph), 7.39 (dm, $^3J_{\text{HH}} = 8.5$ Hz, 2H, Ph), 3.89 (s, 3H, OCH₃). $^{13}\text{C}\{^1\text{H}\}$ NMR (151 MHz, CDCl₃, 298 K): δ = 166.3 (C=O), 139.4 (*i*-Ph), 131.1, 128.8 (Ph), 128.7 (*i*-Ph), 52.3 (OCH₃).

Preparation of 4fa. A methanol suspension (0.65 mL, 16 mmol, 16 equiv) of 3-methylbenzaldehyde (0.12 g, 1 mmol, 1 equiv) and (NH₄)₂S₂O₈ (0.35 g, 1.5 mmol, 1.5 equiv) was stirred at 60 °C for 3.0 h. After cooling to room temperature, distilled water (10 mL) was used to dissolve the solid and the product was extracted by ethyl acetate (3 × 10 mL). The combined organic extract was concentrated and then purified by column chromatography on silica gel (petroleum ether/ethyl acetate 20:1) provided **4fa** in a yield of 87%. ^1H NMR (600 MHz, CDCl₃, 298 K) δ = 7.85 (br s, 1H, *o*-Ph), 7.83 (dm, $^3J_{\text{HH}} = 7.5$ Hz, 1H, *o'*-Ph), 7.33 (dm, $^3J_{\text{HH}} = 7.8$ Hz, 1H, *p*-Ph), 7.30 (tm, $^3J_{\text{HH}}$

= 7.5 Hz, 1H, *m'*-Ph), 3.89 (s, 3H, OCH₃), 2.37 (s, 3H, CH₃). $^{13}\text{C}\{^1\text{H}\}$ NMR (151 MHz, CDCl₃, 298 K): δ = 167.1 (C=O), 138.0 (*m*-Ph), 133.6 (*p*-Ph), 130.1 (*i*-Ph and *o*-Ph), 128.2 (*m'*-Ph), 126.7 (*o'*-Ph), 51.9 (OCH₃), 21.1 (CH₃).

Preparation of 4ab. An ethanol suspension (0.74 g, 16 mmol, 16 equiv) of benzaldehyde (0.11 g, 1 mmol, 1 equiv) and (NH₄)₂S₂O₈ (0.35 g, 1.5 mmol, 1.5 equiv) was stirred at 60 °C for 24 h. After cooling to room temperature, distilled water (10 mL) was used to dissolve the solid and the product was extracted by ethyl acetate (3 × 10 mL). The combined organic extract was concentrated and then purified by column chromatography on silica gel (petroleum ether/ethyl acetate 30:1) provided **4ab** in a yield of 98%. ^1H NMR (600 MHz, CDCl₃, 298 K): δ = 8.05 (dm, $^3J_{\text{HH}} = 8.4$ Hz, 2H, Ph), 7.53 (tm, $^3J_{\text{HH}} = 7.5$ Hz, 1H, *p*-Ph), 7.42 (ddm, $^3J_{\text{HH}} = 8.4$ Hz, $^3J_{\text{HH}} = 7.5$ Hz, 2H, Ph), 4.37 (q, $^3J_{\text{HH}} = 7.1$ Hz, 2H, CH₂^{Et}), 1.39 (t, $^3J_{\text{HH}} = 7.1$ Hz, 3H, CH₃^{Et}). $^{13}\text{C}\{^1\text{H}\}$ NMR (151 MHz, CDCl₃, 298 K): δ = 166.7 (C=O), 132.9 (Ph), 130.6 (*i*-Ph), 129.6, 128.4 (Ph), 61.0 (OCH₂), 14.4 (CH₃^{Et}).

Preparation of 4ac. A butanol suspension (1.19 g, 16 mmol, 16 equiv) of benzaldehyde (0.11 g, 1 mmol, 1 equiv) and (NH₄)₂S₂O₈ (0.35 g, 1.5 mmol, 1.5 equiv) was stirred at 60 °C for 48 h. After cooling to room temperature, distilled water (10 mL) was used to dissolve the solid and the product was extracted by ethyl acetate (3 × 10 mL). The combined organic extract was concentrated and then purified by column chromatography on silica gel (petroleum ether/ethyl acetate 30:1) provided **4ac** in a yield of 99%. ^1H NMR (600 MHz, CDCl₃, 298 K): δ = 8.05 (dm, $^3J_{\text{HH}} = 7.5$ Hz, 2H, Ph), 7.54 (tm, $^3J_{\text{HH}} = 7.4$ Hz, 1H, *p*-Ph), 7.43 (ddm, $^3J_{\text{HH}} = 7.5$ Hz, $^3J_{\text{HH}} = 7.4$ Hz, 2H, Ph), 4.33 (t, $^3J_{\text{HH}} = 6.6$ Hz, 2H, OCH₂^{Bu}), 1.75 (m, 2H, CH₂^{Bu}), 1.48 (m, 2H, CH₂^{Bu}), 0.98 ($^3J_{\text{HH}} = 7.3$ Hz, 3H, CH₃^{Bu}). $^{13}\text{C}\{^1\text{H}\}$ NMR (151 MHz, CDCl₃, 298 K): δ = 166.7 (C=O), 132.8 (Ph), 130.6 (*i*-Ph), 129.6, 128.4 (Ph), 64.9 (OCH₂), 30.9, 19.4 (CH₂^{Bu}), 13.8 (CH₃^{Bu}).

Preparation of 4ad. An isopropanol suspension (0.96 g, 16 mmol, 16 equiv) of benzaldehyde (0.11 g, 1 mmol, 1 equiv) and (NH₄)₂S₂O₈ (0.35 g, 1.5 mmol, 1.5 equiv) was stirred at 60 °C for 24 h. After cooling to room temperature, distilled water (10 mL) was used to dissolve the solid and the product was extracted by ethyl acetate (3 × 10 mL). The combined organic extract was concentrated and then purified by column chromatography on silica gel (petroleum ether/ethyl acetate 30:1) provided **4ad** in a yield of 85%. ^1H NMR (600 MHz, CDCl₃, 298 K): δ = 8.05 (dm, $^3J_{\text{HH}} = 7.6$ Hz, 2H, Ph), 7.53 (tm, $^3J_{\text{HH}} = 7.4$ Hz, 1H, *p*-Ph), 7.42 (ddm, $^3J_{\text{HH}} = 7.6$ Hz, $^3J_{\text{HH}} = 7.4$ Hz, 2H, Ph), 5.26 (hept, $^3J_{\text{HH}} = 6.3$ Hz, 1H, CH^{iPr}), 1.37 (d, $^3J_{\text{HH}} = 6.3$ Hz, 6H, CH₃^{iPr}). $^{13}\text{C}\{^1\text{H}\}$ NMR (151 MHz, CDCl₃, 298 K): δ = 166.2 (C=O), 132.7 (Ph), 131.0 (*i*-Ph), 129.6, 128.3 (Ph), 68.4 (CH^{iPr}), 22.0 (CH₃^{iPr}).

Preparation of 4ae. A *tert*-butanol suspension (1.19 g, 16 mmol, 16 equiv) of benzaldehyde (0.11 g, 1 mmol, 1 equiv) and (NH₄)₂S₂O₈ (0.35 g, 1.5 mmol, 1.5 equiv) was stirred at 60 °C for 16 h. After cooling to room temperature, distilled water (10 mL) was used to dissolve the solid and the product was extracted by ethyl acetate (3 × 10 mL). The combined organic extract was concentrated and then purified by preparative TLC (petroleum ether/ethyl acetate 30:1) provided **4ae** in a yield of 21%. ^1H NMR (600 MHz, CDCl₃, 298 K): δ = 7.99 (dm, $^3J_{\text{HH}} = 7.2$ Hz, 2H, Ph), 7.52 (tm, $^3J_{\text{HH}} = 7.4$ Hz, 1H, *p*-Ph), 7.41 (ddm, $^3J_{\text{HH}} = 7.6$ Hz, $^3J_{\text{HH}} = 7.4$ Hz, 2H, Ph), 1.60 (s, 9H, 3 × CH₃^{t-Bu}). $^{13}\text{C}\{^1\text{H}\}$ NMR (151 MHz, CDCl₃, 298 K): δ = 165.9 (C=O), 132.5 (Ph), 132.2 (*i*-Ph), 129.5, 128.3 (*o*,*m*-Ph), 81.1 (Cq^{t-Bu}), 28.3 (CH₃^{t-Bu}).

Preparation of 4af. A benzyl alcohol suspension (1.73 g, 16 mmol, 16 equiv) of benzaldehyde (0.11 g, 1 mmol, 1 equiv) and (NH₄)₂S₂O₈ (0.35 g, 1.5 mmol, 1.5 equiv) was stirred at 60 °C for 8 h. After cooling to room temperature, distilled water (10 mL) was used to dissolve the solid and the product was extracted by ethyl acetate (3 × 10 mL). The combined organic extract was concentrated and then purified by preparative TLC (petroleum ether/ethyl acetate 30:1) provided **4af** in a yield of 82%. ^1H NMR (600 MHz, CDCl₃, 298 K): δ = 8.09 (dm, $^3J_{\text{HH}} = 7.1$ Hz, 2H, *o*-Ph), 7.56 (m, 1H, *p*-Ph), 7.46 (dm, $^3J_{\text{HH}} = 7.5$ Hz,

2H, *o*-Ph), 7.44 (m, 2H, *m*-Ph), 7.40 (m, 2H, *m*-Ph), 7.36 (m, 1H, *p*-Ph), 5.38 (s, 2H, CH₂). ¹³C{¹H} NMR (151 MHz, CDCl₃, 298 K): δ = 166.6 (C=O), 136.2 (*i*-Ph), 133.2 (*p*-Ph), 130.3 (*i*-Ph), 129.8 (*o*/*m*-Ph), 128.7 (*o*/*m*-Ph), 128.5 (*o*/*m*-Ph), 128.4 (*p*-Ph), 128.3 (*o*/*m*-Ph), 66.8 (CH₂).

■ ASSOCIATED CONTENT

📄 Supporting Information

The Supporting Information is available free of charge on the ACS Publications website at DOI: 10.1021/acs.joc.6b02775.

Characterization and comparison of the ionic oxidants and intermediate, oxidants screening, Hammett studies, radical spin-trap experiment, experiments trapping the transient MeOSO₃⁻, NMR study of the reaction rate of MeOH with **1a** or **6**, theoretic calculations, ¹H and ¹³C NMR spectra for all synthesized new compounds (PDF) Single-crystal X-ray data for **1a**, **1d**, and **6d** (CIF)

■ AUTHOR INFORMATION

Corresponding Authors

*E-Mail: bhxu@ipe.ac.cn

*E-Mail: sjzhang@ipe.ac.cn

ORCID

Bao-Hua Xu: 0000-0002-7222-4383

Suo-Jiang Zhang: 0000-0002-9397-954X

Author Contributions

^{||}X.-Q.Y. and H.-Y.H. contributed equally to the quantum chemical calculations

Notes

The authors declare no competing financial interest.

■ ACKNOWLEDGMENTS

We thank Dr. Yukio Mizuta and Dr. Yue-Qi Ye at JEOL RESONANCE Inc. for the kind simulation of ESR spectra. And financial supports by 973 Program (No. 2015CB251401), Key Program of National Natural Science Foundation of China (No. 91434203), National Natural Science Foundation of China (No. 21476240 and 21406230), Instrument Developing Project of the Chinese Academy of Sciences (No. YZ201521) and CAS 100-Talent Program (2014), are gratefully acknowledged.

■ REFERENCES

- (1) Otera, J. *Esterification: Methods, Reactions, and Applications*; Wiley-VCH: Weinheim, 2003.
- (2) Larock, R. C. *Comprehensive organic transformations: a guide to functional group preparations*; Wiley-vch: New York, 1999.
- (3) Selected reviews see: (a) Tang, S.; Yuan, J.; Liu, C.; Lei, A. *Dalton Trans.* **2014**, 43, 13460–13470. (b) Ekoue-Kovi, K.; Wolf, C. *Chem. - Eur. J.* **2008**, 14, 6302–6315.
- (4) Selected articles for oxidative esterification without catalysis: (a) Tank, R.; Pathak, U.; Vimal, M.; Bhattacharyya, S.; Pandey, L. K. *Green Chem.* **2011**, 13, 3350–3354. (b) Verma, A. K.; Aggarwal, T.; Rustagi, V.; Larock, R. C. *Chem. Commun.* **2010**, 46, 4064–4066. (c) Reddy, K. R.; Venkateshwar, M.; Maheswari, C. U.; Prashanthi, S. *Synth. Commun.* **2009**, 40, 186–195. (d) Rajbongshi, K. K.; Sarma, M. J.; Phukan, P. *Tetrahedron Lett.* **2014**, 55, 5358–5360.
- (5) Selected articles for metal catalyzed oxidative esterification of aldehydes through hemiacetal process: (a) Liu, C.; Tang, S.; Zheng, L.; Liu, D.; Zhang, H.; Lei, A. *Angew. Chem., Int. Ed.* **2012**, 51, 5662–5666. (b) Yoo, W.-J.; Li, C.-J. *Tetrahedron Lett.* **2007**, 48, 1033–1035. (c) Lerebours, R.; Wolf, C. *J. Am. Chem. Soc.* **2006**, 128, 13052–13053. (d) Tschaen, B. A.; Schmink, J. R.; Molander, G. A. *Org. Lett.*

2013, 15, 500–503. (e) Feng, J.-B.; Gong, J.-L.; Li, Q.; Wu, X.-F. *Tetrahedron Lett.* **2014**, 55, 1657–1659. (f) Guo, Y.-F.; Xu, B.-H.; Li, T.; Wang, L.; Zhang, S.-J. *Org. Chem. Front.* **2016**, 3, 47–52.

(6) Selected articles for metal catalyzed oxidative esterification of alcohols through hemiacetal process: (a) Liu, C.; Wang, J.; Meng, L.; Deng, Y.; Li, Y.; Lei, A. *Angew. Chem., Int. Ed.* **2011**, 50, 5144–5148. (b) Gowrisankar, S.; Neumann, H.; Beller, M. *Angew. Chem., Int. Ed.* **2011**, 50, 5139–5143. (c) Wu, X.-F. *Chem. - Eur. J.* **2012**, 18, 8912–8915. (d) Bai, X.-F.; Lai, G.-Q.; Xia, C.-G.; Xu, L.-W.; Ye, F.; Zheng, L.-S. *Chem. Commun.* **2012**, 48, 8592–8594. (e) Wang, L.; Li, J.; Dai, W.; Lv, Y.; Zhang, Y.; Gao, S. *Green Chem.* **2014**, 16, 2164–2173.

(7) Selected articles for metal catalyzed Tishchenko reaction through hemiacetal process: (a) Andrea, T.; Barnea, E.; Eisen, M. S. *J. Am. Chem. Soc.* **2008**, 130, 2454–2455. (b) Day, B. M.; Mansfield, N. E.; Coles, M. P.; Hitchcock, P. B. *Chem. Commun.* **2011**, 47, 4995–4997. (c) Tejel, C.; Ciriano, M. A.; Passarelli, V. *Chem. - Eur. J.* **2011**, 17, 91–95.

(8) Selected articles for organocatalytic oxidative esterification through carbonyl group activation: (a) Delany, E. G.; Fagan, C. L.; Gundala, S.; Zeidler, K.; Connon, S. J. *Chem. Commun.* **2013**, 49, 6513–6515. (b) Sarkar, S. D.; Grimme, S.; Studer, A. *J. Am. Chem. Soc.* **2010**, 132, 1190–1191. (c) Berry, M. T.; Castrejon, D.; Hein, J. E. *Org. Lett.* **2014**, 16, 3676–3679. (d) Tan, B. B.; Toda, N.; Barbas, C. F. *Angew. Chem., Int. Ed.* **2012**, 51, 12538–12541.

(9) Selected articles for esterification through C-H activation/C-O coupling: (a) Whittaker, A. M.; Dong, V. M. *Angew. Chem., Int. Ed.* **2015**, 54, 1312–1315. (b) Kumar, G. S.; Maheswari, C. U.; Kumar, R. A.; Kantam, M. L.; Reddy, K. R. *Angew. Chem., Int. Ed.* **2011**, 50, 11748–11751. (c) Tanaka, K.; Fu, G. C. *Angew. Chem., Int. Ed.* **2002**, 41, 1607–1609.

(10) (a) Chatgililoglu, C.; Crich, D.; Komatsu, M.; Ryu, I. *Chem. Rev.* **1999**, 99, 1991–2070. (b) Beck, R.; Floerke, U.; Klein, H.-F. *Inorg. Chem.* **2009**, 48, 1416–1422. (c) Watanabe, E.; Kaiho, A.; Kusama, H.; Iwasawa, N. *J. Am. Chem. Soc.* **2013**, 135, 11744–11747.

(11) (a) Sharma, V. B.; Jain, S. L.; Sain, B. *Tetrahedron Lett.* **2003**, 44, 383. (b) Murahashi, S. I.; Naota, T.; Hirai, N. *J. Org. Chem.* **1993**, 58, 7318. (c) Tung, H. C.; Sawyer, D. T. *J. Am. Chem. Soc.* **1990**, 112, 8214. (d) Zhang, G.; Vasudevan, K. V.; Scott, B. L.; Hanson, S. K. *J. Am. Chem. Soc.* **2013**, 135, 8668. (e) Sobkowiak, A.; Sawyer, D. T. *J. Am. Chem. Soc.* **1991**, 113, 9520.

(12) Liu, C.; Liu, D.; Lei, A. *Acc. Chem. Res.* **2014**, 47, 3459–3470.

(13) Selected reviews see: (a) Wilmarth, W. K.; Schwartz, N.; Giuliano, C. R. *Coord. Chem. Rev.* **1983**, 51, 243–265. (b) Minisci, F.; Citterio, A.; Giordano, C. *Acc. Chem. Res.* **1983**, 16, 27–32.

(14) Selected articles in biochemistry: (a) Gau, B. C.; Chen, H.; Zhang, Y.; Gross, M. L. *Anal. Chem.* **2010**, 82, 7821–7827. In synthesis: (b) Lu, Q.; Liu, C.; Huang, Z.; Ma, Y.; Zhang, J.; Lei, A. *Chem. Commun.* **2014**, 50, 14101–14104. (c) Wei, Y.; Tang, J.; Cong, X.; Zeng, X. *Green Chem.* **2013**, 15, 3165–3169. (d) Patel, N. R.; Flowers, R. A. *J. Am. Chem. Soc.* **2013**, 135, 4672–4675. (e) Yan, K.; Yang, D.; Wei, W.; Wang, F.; Shuai, Y.; Li, Q.; Wang, H. *J. Org. Chem.* **2015**, 80, 1550–1556. In materials: (f) Bober, P.; Stejskal, J.; Trchova, M.; Prokes, J. *Polymer* **2011**, 52, 5947–5952.

(15) (a) Zemel, H.; Fessenden, R. W. *J. Phys. Chem.* **1975**, 79, 1419–1427. (b) Schuler, R. H.; Neta, P.; Zemel, H.; Fessenden, R. W. *J. Am. Chem. Soc.* **1976**, 98, 3825–3831. (c) Neta, P.; Madhavan, V.; Zemel, H.; Fessenden, R. W. *J. Am. Chem. Soc.* **1977**, 99, 163–164.

(16) (a) Wiberg, K. B. *J. Am. Chem. Soc.* **1959**, 81, 252–253. (b) Clifton, C. L.; Huie, R. E. *Int. J. Chem. Kinet.* **1989**, 21, 677–687. (c) George, C.; El Rassy, H.; Chovelon, J. M. *Int. J. Chem. Kinet.* **2001**, 33, 539–547. (d) Khursan, S. L.; Semes'ko, D. G.; Teregulova, A. N.; Safullin, R. L. *Kinet. Catal.* **2008**, 49, 202–211.

(17) (a) Tsujimoto, S.; Iwahama, T.; Sakaguchi, S.; Ishii, Y. *Chem. Commun.* **2001**, 2352–2353. (b) Wang, J.; Liu, C.; Yuan, J.; Lei, A. *Angew. Chem., Int. Ed.* **2013**, 52, 2256–2259. (c) Yang, W.-C.; Weng, S.-S.; Ramasamy, A.; Rajeshwaren, G.; Liao, Y.-Y.; Chen, C.-T. *Org. Biomol. Chem.* **2015**, 13, 2385–2392.

(18) Lin, M.; Sen, A. *J. Chem. Soc., Chem. Commun.* **1992**, 12, 892–893.

- (19) Staško, A.; Brezová, V.; Liptáková, M.; Šavel, J. *Magn. Reson. Chem.* **2000**, *38*, 957–962.
- (20) Luo, Y. R. *Handbook of bond dissociation energies in organic compounds*; CRC Press, 2003.
- (21) (a) Shi, S.; Kong, A.; Zhao, X.; Zhang, Q.; Shan, Y. *Eur. J. Inorg. Chem.* **2010**, *2010*, 2283–2289. (b) Travis, B. R.; Sivakumar, M.; Hollist, G. O.; Borhan, B. *Org. Lett.* **2003**, *5*, 1031–1034.
- (22) Gall, J. F.; Church, G. L.; Brown, R. L. *J. Phys. Chem.* **1943**, *47*, 645–649.
- (23) Apelblat, A.; Korin, E.; Manzurola, E. *J. Chem. Thermodyn.* **2001**, *33*, 61–69.
- (24) Yang, S. G.; Hwang, J. P.; Park, M. Y.; Lee, K.; Kim, Y. H. *Tetrahedron* **2007**, *63*, 5184–5188.
- (25) (a) Liu, Z.; Zhang, J.; Chen, S.; Shi, E.; Xu, Y.; Wan, X. *Angew. Chem., Int. Ed.* **2012**, *51*, 3231–3235. (b) Cadoni, R.; Porcheddu, A.; Giacomelli, G.; De Luca, L. *Org. Lett.* **2012**, *14*, 5014–5017. (c) Liu, W.; Li, Y.; Liu, K.; Li, Z. *J. Am. Chem. Soc.* **2011**, *133*, 10756–10759.
- (26) Guo, Q.; Qian, S. Y.; Mason, R. P. *J. Am. Soc. Mass Spectrom.* **2003**, *14*, 862–871.
- (27) Nishihara, A.; Kubota, I. *J. Org. Chem.* **1968**, *33*, 2525–2526.
- (28) (a) da Silva, E. T.; Câmara, C. A.; Antunes, O. A. C.; Barreiro, E. J.; Fraga, C. A. M. *Synth. Commun.* **2008**, *38*, 784–788. (b) Chen, S.; Foss, F. W. *Org. Lett.* **2012**, *14*, 5150–5153.
- (29) Kolthoff, I. M.; Miller, I. K. *J. Am. Chem. Soc.* **1951**, *73*, 3055–3059.
- (30) Bartlett, P. D.; Cotman, J. D. *J. Am. Chem. Soc.* **1949**, *71*, 1419–1422.